

Effect of Landau-Zener tunneling on the conductivity of a two-dimensional electron gas

V. R. Gushchin

Moscow Physicotechnical Institute, 140160 Zhukovskii, Moscow Oblast, Russia

(Submitted 14 July 1993)

Zh. Eksp. Teor. Fiz. 105, 1323–1341 (May 1994)

A two-dimensional semiconductor heterostructure consisting of two asymmetric quantum wells separated by a potential barrier is studied. The conductivity of this structure in a weak electric field directed parallel to the walls of the quantum wells is investigated theoretically. It is shown that when neutral scattering centers are present in one of the wells, the current-voltage characteristic contains a section with negative differential resistance, whose existence depends strongly on the geometric parameters of the heterostructure. This section is associated with Landau-Zener tunneling in a longitudinal electric field.

1. INTRODUCTION

There are a large number of theoretical and experimental works on tunneling in low-dimensional quantum systems in semiconductor heterostructures. These processes significantly influence the electric and optical properties of the structures. If two quantum wells with close energy levels are separated by a potential barrier, then a slight variation of the external electric field can substantially change the wave functions and give rise to a displacement of charge carriers in real space. This fact was employed in Ref. 1 to model IR absorption and in Refs. 2–4 to investigate exciton tunneling.

Another parameter that depends strongly on the degree of overlap of the wave functions is the conductivity. The possibility of controlling the ohmic resistance of a resonance-tunneling heterostructure was investigated theoretically in Ref. 5. Control was achieved both by varying the intensity of the transverse electric field and by the position of the Fermi level. Conductivity modulation is effective in this case if the electron scattering rate in different wells is significantly different. The electron mobility is observed to drop sharply near a tunneling resonance. Bistability, a highly nonlinear phenomenon, can also be observed in a transverse electric field.⁶

An important phenomenon neglected in Ref. 5 is Landau-Zener tunneling^{7–10} in a longitudinal electric field. As shown in Ref. 10, this process appears in the ballistic regime when electrons accelerated in an electric field pass through the resonance tunneling point. In this case there is an aperiodic transfer (in contrast to transfers which are periodic in time and space^{11–12}) of electrons from one quantum well to another. Landau-Zener tunneling appears only in asymmetric quantum wells with different effective mass under stringent restrictions on the dimensions of the wells and the barrier. This process is nondissipative and cannot by itself result in the appearance of ohmic resistance. The process results from the scattering of charge carriers by phonons and impurities localized in one of the quantum wells. In order that scattering not impede tunneling, however, the relaxation time must be longer than the electron transition time through the resonance tunneling zone. For this reason we employed in this work the model

of a resonance impurity, the probability of scattering by which is significant for low electron kinetic energies. The impurity scattering energies must be far from the resonance tunneling energy, which itself must be less than the energy $\hbar\omega_0$ of polar optical phonons.

2. FORMULATION OF THE PROBLEM

We study electron motion in a semiconductor heterostructure consisting of a pure GaAs layer 1 with thickness b_1 , an $\text{Al}_x\text{Ga}_{1-x}\text{As}$ layer 2 with thickness b_2 , and a middle layer 3 with an elevated aluminum concentration and thickness b_3 . An electric field E is oriented parallel to the interfaces between the layers. The x axis is oriented along the electric field, the z axis is perpendicular to the heterostructure, and the y axis is perpendicular to the x and z axes. The origin of the coordinate system is located at the outer boundary of layer 1. All three layers are located in an infinitely deep potential well. The electron potential energy will then have the form shown in Fig. 1. The complete wave function satisfies the time-dependent Schrödinger equation

$$i\hbar \frac{\partial \Psi}{\partial t} = (\hat{H}_e + \hat{H}_{\text{ph}} + \hat{H}_{e-\text{ph}} + \hat{H}_{e-\text{imp}}) \Psi, \quad (1)$$

where Ψ is the full time-dependent wave function, which depends on the three coordinates of the electron and the normal coordinates of the crystal lattice. The Hamiltonian operators \hat{H}_e and \hat{H}_{ph} operate only on the electron and phonon parts of the wave function, $\hat{H}_{e-\text{ph}}$ is the electron-phonon interaction Hamiltonian, and $\hat{H}_{e-\text{imp}}$ describes electron scattering by the impurity. In this paper the electron-electron interaction is not considered. Treating $\hat{H}_{e-\text{ph}}$ and $\hat{H}_{e-\text{imp}}$ as first-order perturbations, we seek an unperturbed solution in the form $\Psi = \Psi_e \Psi_{\text{ph}}$. For the electronic component we have

$$i\hbar \frac{\partial \Psi_e}{\partial t} = \hat{H}_e \Psi_e, \quad (2)$$

where

$$\hat{H}_e = -\frac{\hbar^2}{2} \text{div} \frac{\nabla}{m} + U(z) - eE_x x, \quad (3)$$

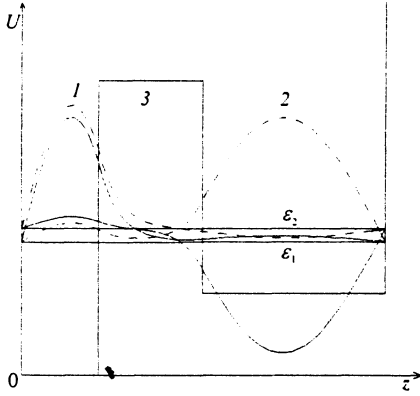


FIG. 1. Overlap of wave functions for a double-well potential [$k=0$ (solid curve) and $2.7 \cdot 10^6 \text{ cm}^{-1}$ (dashed curve)].

the electron effective mass m depends only on z , and E_x is the longitudinal electric field.

We represent the wave function as a product of an amplitude function and an exponential:

$$\Psi_e(x, y, z, t) = \Psi_0(z, t) \exp\left(ik_{0x}x + ik_y y + \frac{i}{\hbar} eE_x x t\right). \quad (4)$$

As shown in Ref. 10, a wave packet consisting of any solution of Eqs. (2) and (3) can be constructed from these solutions. The function Ψ_0 satisfies the wave equation

$$i\hbar \frac{\partial \Psi_0}{\partial t} = \hat{H}_0 \Psi_0, \quad (5)$$

where

$$\hat{H}_0 = -\frac{\hbar^2}{2} \frac{\partial}{\partial z} \frac{1}{m} \frac{\partial}{\partial z} + U + \frac{\hbar^2 k^2}{2m}. \quad (6)$$

The wave vector $\mathbf{k} = (k_x, k_y)$ determines the semiclassical motion of an electron in the (xy) plane. We obtain for the projections of \mathbf{k}

$$k_x = k_{0x} + \frac{eE_x}{\hbar} t, \quad k_y = \text{const}. \quad (7)$$

The Hamiltonian \hat{H}_0 is thus explicitly time dependent. We seek the solution of the problem (5) in the form of an expansion in the eigenfunctions of the operator \hat{H}_0 , taken at a fixed moment in time, $\hat{H}_0 \psi_n = \varepsilon_n \psi_n$:

$$\Psi_0 = \sum_n C_n(t) \psi_n(z, t) \exp\left[-\frac{i}{\hbar} \int_{t_*}^t \varepsilon_n(t') dt'\right]. \quad (8)$$

The free parameter t_* will be determined in Sec. 3. Using Eqs. (5)–(8), we obtain a system of differential equations for the constants C_n as a function of time:

$$\dot{C}_n = \sum_l W_{nl} \exp\left[\frac{i}{\hbar} \int_{t_*}^t (\varepsilon_n - \varepsilon_l) dt'\right] C_l. \quad (9)$$

The wave functions ψ_n correspond to the stationary states of an electron with wave vector \mathbf{k} in the absence of an electric field, and the index n enumerates the size-

quantization subbands. The coefficients W_{nl} determine the rate of Landau-Zener tunneling between subbands:

$$W_{nl} = - \int \psi_n^* \frac{\partial \psi_l}{\partial t} dz = \frac{\hbar k_x e E_x}{\varepsilon_n - \varepsilon_l} \int \frac{\psi_n^* \psi_l}{m} dz. \quad (10)$$

Impurity scattering and electron-phonon interaction are usually treated on the basis of Fermi's golden rule. This rule gives the transition rate of a quantum system from the stationary state $|i\rangle$ to another stationary state $|f\rangle$:

$$W_{i \rightarrow f} = \frac{2\pi}{\hbar} |\langle f | \hat{H}_{e-\text{ph}} | i \rangle|^2 \delta(\varepsilon_f - \varepsilon_i). \quad (11)$$

Here the initial and final states contain both phonon and electron components of the Ψ function. The crystal is assumed to be in a state of thermodynamic equilibrium at temperature T , and the phonon part of the wave function can be assumed to be stationary. The electron part, however, as follows from Eqs. (7), (10), is definitely nonstationary, provided that $E_x \neq 0$. At any moment in time the state of an electron is given by a superposition of states of the Hamiltonian \hat{H}_0 , i.e., Eq. (11) is inapplicable.

We now introduce a more general formula that is more convenient to use in a kinetic equation. We consider two size-quantization subbands 1 and 2 and define a mixed state as the linear combination $|i\rangle = c_1 |i_1\rangle + c_2 |i_2\rangle$, where $|i_1\rangle$ and $|i_2\rangle$ are electronic states of the Hamiltonian \hat{H}_0 with some wave number k . An equation of the type (9) can be written down for the probability amplitude c_f for finding the quantum system in the final state $|f\rangle$,

$$i\hbar \dot{c}_f = \sum_i \langle f | \hat{H}_{e-\text{ph}} | i \rangle \exp\left[\frac{i}{\hbar} (E_f - E_i) t\right] c_i, \quad (12)$$

and the initial condition at $t=0$:

$$c_1 = C_1, \quad c_2 = C_2, \quad c_f = 0. \quad (13)$$

Here the states $|f\rangle$ and $|i\rangle$ and the energies E_f and E_i contain both electronic and phonon parts, and the constants C_1 and C_2 are taken from the solution (9). Integrating Eq. (12) and calculating

$$W_{i \rightarrow f} = \lim_{t \rightarrow \infty} \frac{d}{dt} |c_f|^2,$$

we obtain an extension of Fermi's golden rule to nonstationary states:

$$\begin{aligned} W_{i \rightarrow f} = & \frac{2\pi}{\hbar} |C_1 \langle f | \hat{H}_{e-\text{ph}} | i_1 \rangle|^2 \delta(E_f - E_1) \\ & + \frac{2\pi}{\hbar} |C_2 \langle f | \hat{H}_{e-\text{ph}} | i_2 \rangle|^2 \delta(E_f - E_2) \\ & + \frac{2\pi}{\hbar} \text{Re} \left\{ C_1 \bar{C}_2 \langle i_2 | \hat{H}_{e-\text{ph}} | f \rangle \langle f | \hat{H}_{e-\text{ph}} | i_1 \rangle \right. \\ & \times \exp\left[\frac{i}{\hbar} (E_2 - E_1) t\right] \left. \right\} [\delta(E_f - E_1) + \delta(E_f \\ & - E_2)]. \end{aligned} \quad (14)$$

If the free-flight time $\tau \gg \hbar/(E_2 - E_1)$, then the last term in this formula can be dropped, since it is rapidly oscillating and averages to zero over time. In our case this can be done if the free-flight time is much longer than the tunneling period between the quantum wells.

3. LANDAU-ZENER TUNNELING

The effective masses in the quantum wells in Fig. 1 are different: $m_1 \neq m_2$. This results in the appearance of a synchronization point and Landau-Zener tunneling. Let k_x increase with time according to Eq. (7). Then the bottom and the energy levels of each well will rise at different rates. For definiteness, let $m_1 < m_2$. The effective potential $U + \hbar^2 k^2/2m$ of the Hamiltonian \hat{H}_0 in region 1 increases more rapidly than in region 2. For this region, if the energy levels of the isolated wells initially satisfy the condition $\varepsilon'_1 < \varepsilon'_2$, then there exists a time t_* after which the inverse inequality $\varepsilon'_1 > \varepsilon'_2$ will hold. Tunneling occurs near t_* .

To investigate the evolution of the wave function at times $t \approx t_*$, it is helpful to consider a more general formulation of the problem. Let $\hat{H}'_1(t)$ and $\hat{H}'_2(t)$ be two nonstationary Hamiltonians. The time dependence might be a consequence of some external action $u(t)$:

$$\hat{H}_n(t) = \hat{H}'_n[u(t)], \quad n=1,2. \quad (15)$$

Here $u(t)$ might correspond, for example, to $k_x^2(t)$ [see Eq. (7)]—an external nonstationary electric or magnetic field. The external perturbation can change the state of these quantum systems. The eigenfunctions and eigenvalues of the Hamiltonians (15) will then depend on the time as a parameter:

$$\hat{H}'_n(t)\psi'_n(t) = \varepsilon'_n(t)\psi'_n(t), \quad n=1,2. \quad (16)$$

Let ψ'_1 and ψ'_2 be normalized to unity, and let them be "almost" orthogonal functions:

$$|\langle \psi'_1(t) | \psi'_2(t) \rangle| < \beta \ll 1. \quad (17)$$

In addition, let there be a Hamiltonian \hat{H}_0 for which ψ'_1 and ψ'_2 are "almost" eigenfunctions

$$\hat{H}_0(t)\psi'_n(t) = \varepsilon'_n(t)\psi'_n(t) + O(\beta), \quad \beta \rightarrow 0, \quad n=1,2, \quad (18)$$

for a pair of quantum wells separated by a tunneling-penetrable potential barrier, where \hat{H}_0 is a double-well Hamiltonian and $\hat{H}_{1,2}$ are single-well Hamiltonians. If the potential barrier is sufficiently high, then the overlap of the functions ψ'_1 and ψ'_2 is small, so that the condition (17) is satisfied.

In this section we consider the time-dependent Schrödinger equation (5) with the Hamiltonian $\hat{H}_0(t) = \hat{H}_0[u(t)]$. We use the two-mode approximation in order to solve this equation. We retain the first two terms in the sum (8), which give the solutions in both wells. The functions ψ_j and ε_j depend on t as a parameter and can be found from the equations

$$\hat{H}_0\psi_j = \varepsilon_j\psi_j, \quad j=1,2. \quad (19)$$

The relations (18) suggest that to within terms of order β , the eigenfunctions [solutions of the problem (19)] can be approximated by eigenfunctions of the Hamiltonians \hat{H}'_n ,

$$\psi_1 = B_1\psi'_1 + B_2\psi'_2, \quad (20)$$

$$\psi_2 = B_3\psi'_1 + B_4\psi'_2.$$

This is true at all t , and the coefficients B_1, \dots, B_4 depend only on the time. In the basis $|\psi'_n\rangle$, the Hamiltonian \hat{H}_0 is a 2×2 matrix:

$$\hat{H}_0 = [\langle \psi'_i | \hat{H}_0 | \psi'_j \rangle] = \begin{bmatrix} \varepsilon'_1 + h_1 & h_{12} \\ h_{12} & \varepsilon'_2 + h_2 \end{bmatrix}.$$

In this matrix h_1 and h_2 are real. In addition, it is assumed that the functions ψ'_n are normalized such that h_{12} is real and positive. It follows from Eq. (18) that h_i and h_{ij} are of order β and are continuous functions of time. In this representation Eq. (19) is a homogeneous system of linear algebraic equations. The dispersion relation that follows from this system has two different solutions:

$$\varepsilon_{1,2} = \frac{1}{2}(\varepsilon'_1 + h_1 + \varepsilon'_2 + h_2 \mp \delta\varepsilon), \quad (21)$$

where

$$\delta\varepsilon = \sqrt{\Delta\varepsilon^2 + 4h_{12}^2}, \quad (22)$$

$$\Delta\varepsilon = \varepsilon'_1 + h_1 - \varepsilon'_2 - h_2. \quad (23)$$

In accordance with Eq. (20), the constants B_1 and B_2 correspond to the minus sign and the constants B_3 and B_4 correspond to the plus sign in Eq. (21):

$$B_1 = B_4 = \sqrt{\frac{1}{2} \left(1 - \frac{\Delta\varepsilon}{\delta\varepsilon} \right)}, \quad B_3 = -B_2 = \sqrt{\frac{1}{2} \left(1 + \frac{\Delta\varepsilon}{\delta\varepsilon} \right)}. \quad (24)$$

Let the time t_* correspond to a tunneling resonance, i.e., $\Delta\varepsilon(t_*) = 0$. In a β neighborhood of the point (ε_*, t_*) in the (ε, t) plane, the eigenvalues of the Hamiltonians \hat{H}'_1 and \hat{H}'_2 occur at the same time: $\varepsilon'_1(t_*) \approx \varepsilon'_2(t_*) \approx \varepsilon_*$, where

$$\varepsilon_* = \frac{1}{2}[\varepsilon'_1(t_*) + h_1(t_*) + \varepsilon'_2(t_*) + h_2(t_*)].$$

For this reason, the point (ε_*, t_*) is said to be a synchronization point. In Fig. 2 this point is located at the intersection of the dashed lines, which, to within the small quantities h_1 and h_2 , display the time dependence of the energy levels $\varepsilon'_1(t)$ and $\varepsilon'_2(t)$. The solid lines correspond to the eigenvalues of the Hamiltonian \hat{H}_0 . It is evident from the figure that the time axis can be divided into three characteristic regions. In the regions 1 and 3 the dispersion relation is virtually identical to the dispersion relation given by the Hamiltonians \hat{H}'_1 and \hat{H}'_2 taken separately. Near the synchronization point 2, a continuous transition occurs from the first to the second dispersion relation and vice versa. The eigenfunctions change similarly. In region 1, $\Delta\varepsilon/\delta\varepsilon \approx -1$, and therefore $B_1 \approx 1$, $B_2 \approx 0$, $B_3 \approx 0$, and $B_4 \approx 1$, i.e., $\psi_1 \approx \psi'_1$ and $\psi_2 \approx \psi'_2$. At the synchronization point, $\Delta\varepsilon = 0$ and $B_1 = -B_2 = B_3 = B_4 = 1/\sqrt{2}$, so that

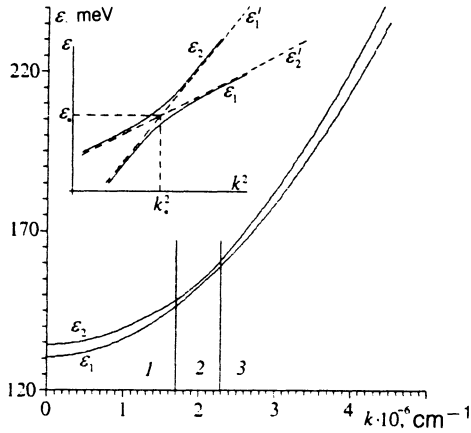


FIG. 2. Size-quantization subbands for a double-well potential. Inset: region 2 on an enlarged scale.

$$\psi_1(t_*) = \frac{1}{\sqrt{2}} (\psi'_1 - \psi'_2),$$

$$\psi_2(t_*) = \frac{1}{\sqrt{2}} (\psi'_1 + \psi'_2).$$
(25)

Similarly, in region 3

$$\Delta\varepsilon/\delta\varepsilon \approx 1, \quad B_1 \approx 0, \quad B_2 \approx -1, \quad B_3 \approx 1, \quad B_4 \approx 0;$$

$$\psi_1 \approx -\psi'_2, \quad \psi_2 \approx \psi'_1.$$

We now consider a quantum system which at time $t=0$ is in the state $|\psi_1\rangle$. As stated above, this state corresponds approximately to the quantum state ψ'_1 . Let the parameter $u(t)$ vary so that the system passes continuously through a neighborhood of the synchronization point. The evolution is determined by the system of ordinary differential equations (9) with initial conditions

$$C_1 = 1, \quad C_2 = 0 \quad \text{at } t=0. \quad (26)$$

We are interested in determining the state of the quantum system in region 3. To simplify the computations, we replace the time by the dimensionless parameter

$$\xi = \frac{\Delta\varepsilon}{\delta\varepsilon_*}, \quad (27)$$

where $\delta\varepsilon_* = \delta\varepsilon(t_*) = 2h_{12}$ is the splitting of the energy levels at the synchronization point. Such a substitution is admissible if $\Delta\varepsilon(t)$ is a monotonic function of time. From Eq. (17) we obtain $\delta\varepsilon_* \sim \beta$, i.e.,

$$\delta\varepsilon_* \ll 1. \quad (28)$$

Thus, near the synchronization point the energy levels are separated by a narrow gap. Hence we obtain an estimate of the derivative of h_{12} :

$$\frac{\partial h_{12}}{\partial \xi} = \delta\varepsilon_* \frac{\partial h_{12}}{\partial (\Delta\varepsilon)} \ll 1, \quad (29)$$

since $\partial h_{12}/\partial(\Delta\varepsilon) \sim \beta$. This estimate enables us to replace h_{12} by a constant in region 2, and to simplify (22) and (24):

$$\delta\varepsilon = \delta\varepsilon_* \sqrt{1 + \xi^2}, \quad (30)$$

$$\pm B_{1,2} = B_{4,3} = \sqrt{\frac{1}{2} \left(1 \mp \frac{\xi}{\sqrt{1 + \xi^2}} \right)}. \quad (31)$$

These expressions can be used to calculate the matrix coefficients W_{nl} in the system of equations (9). We replace the time derivative by a derivative with respect to the variable ξ :

$$\frac{\partial \psi}{\partial t} = \frac{1}{\tau} \frac{\partial \psi}{\partial \xi}, \quad (32)$$

where

$$\frac{1}{\tau} = \frac{d\xi}{dt} = \frac{1}{\delta\varepsilon_*} \frac{\partial \Delta\varepsilon}{\partial t} \quad (33)$$

has the dimensions of time and is a weak function of t or ξ . Next, we assume that the functions ψ_n are real. This is true of the Hamiltonian (6) and many other cases. Then the diagonal elements of the matrix W are strictly equal to zero:

$$\left\langle \psi_n \left| \frac{\partial \psi_n}{\partial t} \right. \right\rangle = \int \psi_n \frac{\partial \psi_n}{\partial t} dV = \frac{1}{2} \frac{\partial}{\partial t} \int \psi_n^2 dV = 0.$$

The cross coefficients to leading order have the form

$$\left\langle \psi_1 \left| \frac{\partial \psi_2}{\partial t} \right. \right\rangle = - \left\langle \psi_2 \left| \frac{\partial \psi_1}{\partial t} \right. \right\rangle = \frac{1}{2\tau(1 + \xi^2)}, \quad (34)$$

where we have dropped terms containing $\partial \psi'_n / \partial \xi \sim \beta$ [which is analogous to Eq. (29)]. Substituting these expressions into Eq. (9), we obtain a simplified form of this system that can be employed near the point of synchronization:

$$\frac{dC_1}{d\xi} = - \frac{C_2}{2(1 + \xi^2)} \exp[-iS(\xi)],$$

$$\frac{dC_2}{d\xi} = \frac{C_1}{2(1 + \xi^2)} \exp[iS(\xi)],$$
(35)

where

$$S(\xi) = \alpha \int_0^\xi \sqrt{1 + \xi'^2} d\xi'$$

$$= \frac{\alpha}{2} [\xi \sqrt{1 + \xi^2} + \ln(\xi + \sqrt{1 + \xi^2})],$$

and α is the only dimensionless constant in this problem:

$$\alpha = \frac{\delta\varepsilon_* \tau}{\hbar}. \quad (36)$$

The value of τ can be calculated at the synchronization point t_* . It can be replaced by a constant in a narrow region 2 if $d \ln \tau / d\xi \ll 1$, or

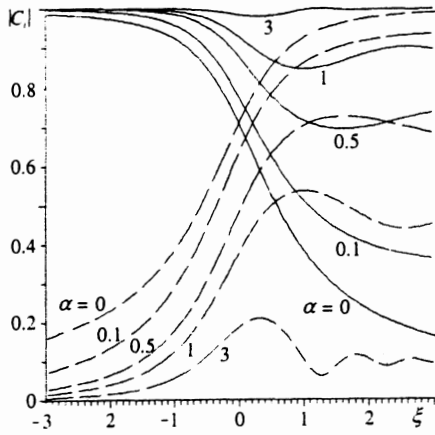


FIG. 3. Probability amplitude for finding the quantum system in states 1 and 2 (solid and dashed lines, respectively) near the synchronization point for different values of the parameter α .

$$\left. \frac{\partial^2 \Delta \varepsilon}{\partial t^2} \right|_{t=t_*} \ll \frac{\delta \varepsilon_*}{\tau^2}. \quad (37)$$

This condition imposes certain constraints on the form of the external action $u(t)$ and the energy spectrum of the problem. When the condition (37) is satisfied, τ is the characteristic traversal time through the resonance-tunneling point.

The system (35) together with the boundary conditions on the left-hand boundary of region 2

$$C_1 = 1, \quad C_2 = 0 \quad \text{at } \xi = -\infty \quad (38)$$

comprise an initial-value problem. According to Eqs. (8), (20), and (31), these initial conditions correspond to finding the quantum system in the state $|\psi'_1\rangle$.

Solutions of this problem for different values of the parameter α are displayed in Fig. 3. It is evident that for $\alpha > 3$, $C_1(\xi) \approx 1$ and $C_2(\xi) \approx 0$. However, the real boundary conditions may differ from (38). When the system (9) is integrated in region 1 from $t=0$ to the left-hand boundary of region 2, arbitrary boundary conditions can arise for the system (35):

$$C_1 = C_{01}, \quad C_2 = C_{02} \quad \text{at } \xi = -\infty. \quad (39)$$

It turns out that the solution of the problem (35) and (39) can be expressed in terms of the solution of the problem (35) and (38). For this we employ the following property: if $[C_1(\xi), C_2(\xi)]$ is a solution of Eq. (35), then $[C_2^*(\xi), -C_1^*(\xi)]$ is also a solution of this system. Let $[Q_{1,\alpha}(\xi), Q_{2,\alpha}(\xi)]$ be a solution of the system (35) with the boundary conditions (38) for some fixed value of the parameter α . Then a solution of the form

$$\begin{aligned} C_1(\xi) &= C_{01}Q_{1,\alpha}(\xi) - C_{02}Q_{2,\alpha}^*(\xi), \\ C_2(\xi) &= C_{01}Q_{2,\alpha}(\xi) + C_{02}Q_{1,\alpha}^*(\xi), \end{aligned} \quad (40)$$

satisfies the system (35) and the conditions (39). Thus the functions $Q_{1,\alpha}(\xi)$ and $Q_{2,\alpha}(\xi)$ contain complete information about all possible solutions of the system (35).

The case $\alpha=0$ corresponds to infinitely rapid traversal of region 2. According to (36) and (33), this case can be approached if the energy gap $\delta \varepsilon_* \ll 1$ and at the same time the external action $u(t)$ varies rapidly in region 2. For $\alpha=0$, the Cauchy problem (35) and (38) has the exact solution

$$Q_{i,0}(\xi) = \sqrt{\frac{1}{2}} \left[1 + (-1)^i \frac{\xi}{\sqrt{1+\xi^2}} \right], \quad i=1,2.$$

Substituting this solution into (8) and using (20), (31), and (40), we find to leading order that $\Psi_0(\xi, z)$ is independent of ξ . In other words, during rapid traversal of the narrow region 2, the quantum state of the system does not change.

The system (35) was integrated numerically for $\alpha \sim 1$. In the limit $\xi \rightarrow \infty$, however, the solutions are approximated well by the analytic expression

$$|Q_{2,\alpha}(\infty)|^2 = \exp\left(-\alpha \frac{\pi}{2}\right). \quad (41)$$

Since the normalization condition

$$|Q_{1,\alpha}(\xi)|^2 + |Q_{2,\alpha}(\xi)|^2 \equiv 1,$$

is satisfied for any ξ and α , $|Q_{1,\alpha}(\infty)|$ can be calculated from this condition. According to Eqs. (8), (20), and (31), $|Q_{1,\alpha}(\infty)|^2$ and $|Q_{2,\alpha}(\infty)|^2$ equal the probability of finding the quantum system in the states $|\psi'_2\rangle$ and $|\psi'_1\rangle$, respectively. Interestingly enough, Eq. (41) yields an error of less than 12% for any $0 < \alpha < \infty$, and it is asymptotically accurate in the limit $\alpha \rightarrow 0$.

Slow traversal of region 2 was studied in detail in Ref. 10, and corresponds to the limit of large α . The formula for $Q_{2,\alpha}(\infty)$ has the form

$$|Q_{2,\alpha}(\infty)|^2 = \frac{\pi^2}{9} \exp\left(-\alpha \frac{\pi}{2}\right), \quad \alpha \rightarrow \infty, \quad (42)$$

which differs from Eq. (41) only by a factor close to unity.

Let $P_{1 \rightarrow 1} = |Q_{2,\alpha}(\infty)|^2$ be the probability of finding the quantum system in state $|\psi'_1\rangle$ after traversal of region 2 under the condition that earlier the system was in the same state. Using Eq. (36) we obtain

$$P_{1 \rightarrow 1} = \exp\left(-\frac{\pi \delta \varepsilon_* \tau}{2\hbar}\right). \quad (43)$$

By virtue of the symmetry of the system of differential equations (35), we have $P_{2 \rightarrow 2} = P_{1 \rightarrow 1}$, $P_{1 \rightarrow 2} = P_{2 \rightarrow 1} = 1 - P_{1 \rightarrow 1}$. Since in this section we did not employ a specific type of Hamiltonian \hat{H}_0 , the last expression is universal and is applicable to any two weakly coupled quantum systems in a small neighborhood of the synchronization point.

4. SCATTERING OF QUASI-TWO-DIMENSIONAL ELECTRONS IN A DOUBLE-WELL HETEROSTRUCTURE

As shown above, a longitudinal electric field causes nonstationary quantum states to appear continually. In addition, according to (9) and (34), the rate of appearance

of these states is greatest near the resonance tunneling point. Dropping the last term in Eq. (14), we obtain the transition rate out of a nonstationary state, which is determined by Fermi's golden rule and the probabilities of finding an electron in the two stationary states.

In this section we study electron scattering by polar optical phonons, acoustic phonons, and impurities. These questions are investigated in detail in Ref. 13 for single- and multiple-well potentials in an external transverse electric field. In contrast to Ref. 13, we shall not assume that the subbands are parabolic. This assumption is inapplicable if a synchronization point exists.

We represent the electron-phonon Hamiltonian as a sum of Hamiltonians for polar optical and acoustic phonons:

$$\hat{H}_{e-ph} = \hat{H}_{e-po} + \hat{H}_{e-ac}.$$

Since the interaction of phonons and electrons is governed by longitudinal oscillations,¹⁴ we retain in these Hamiltonians only the longitudinal optical and acoustic phonons. In a weak electric field, the electrons in the Γ valley of the conduction band are located close to the center of the Brillouin zone, and for this reason here we employ the long-wavelength phonon approximation. Following Ref. 15, we write \hat{H}_{e-po} in the form

$$\hat{H}_{e-po} = -e \sqrt{\frac{2\pi\hbar\omega_0}{V\bar{\epsilon}}} \sum_{\mathbf{q}} \frac{e^{i\mathbf{q}\mathbf{r}}}{q} (\hat{b}_{\mathbf{q}} - \hat{b}_{-\mathbf{q}}^{\dagger}), \quad (44)$$

where $\hbar\omega_0$ and \mathbf{q} are, respectively, the energy and wave vector of longitudinal optical phonons; $\hat{b}_{\mathbf{q}}$ and $\hat{b}_{\mathbf{q}}^{\dagger}$ are the phonon creation and annihilation operators; $\bar{\epsilon}^{-1} = \epsilon_{\infty}^{-1} - \epsilon_0^{-1}$, where ϵ_{∞} and ϵ_0 are the high-frequency and static dielectric constants; and, V is the volume of the crystal. The summation extends over the entire Brillouin zone. We give the initial and final states as products of the electronic part ψ and the phonon parts ϕ , corresponding to phonon occupation numbers $N_{\mathbf{q}}$:

$$\Psi_i = \psi_i \prod_{\mathbf{q}} \phi_{N_{\mathbf{q}}}, \quad \Psi_f = \psi_f \prod_{\mathbf{q}} \phi_{N_{\mathbf{q}}}.$$

Using the property $\hat{b}_{\mathbf{q}}\phi_{N_{\mathbf{q}}} = \sqrt{N_{\mathbf{q}}}\phi_{N_{\mathbf{q}}-1}$, $\hat{b}_{\mathbf{q}}^{\dagger}\phi_{N_{\mathbf{q}}} = \sqrt{N_{\mathbf{q}}+1}\phi_{N_{\mathbf{q}}+1}$, as well as the orthonormality of the phonon eigenfunctions, we obtain from Eqs. (44) and (11)

$$W_{i \rightarrow f} = \frac{4\pi^2 e^2 \omega_0}{V\bar{\epsilon}} \sum_{\mathbf{q}} \frac{1}{q^2} |\langle \psi_f | e^{i\mathbf{q}\mathbf{r}} | \psi_i \rangle|^2 [N_{\mathbf{q}} \delta(\epsilon_i - \epsilon_f + \hbar\omega_0) + (N_{\mathbf{q}} + 1) \delta(\epsilon_i - \epsilon_f - \hbar\omega_0)]. \quad (45)$$

For a crystal in thermodynamic equilibrium, we take for $N_{\mathbf{q}}$ the Bose-Einstein distribution function:

$$N_{\mathbf{q}}^{-1} = \exp\left(\frac{\hbar\omega_0}{k_B T}\right) - 1,$$

where k_B is Boltzmann's constant. We note that the two-dimensional wave vector \mathbf{k}_f of the final state is determined completely by the wave vector \mathbf{k}_i of the initial state, the scattering angle θ , and the energy and quasimomentum conservation laws (the quasimomentum conservation law

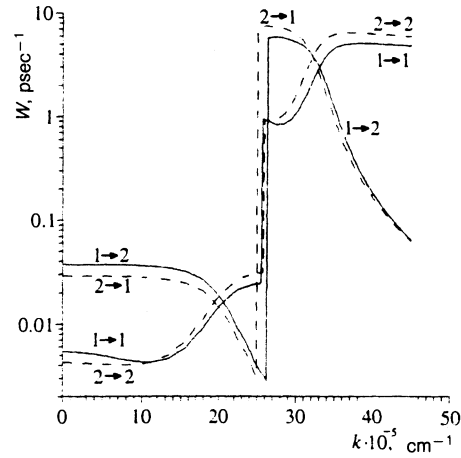


FIG. 4. Transition rates between subbands with electron scattering by polar optical phonons.

is applied in a plane parallel to the walls of the quantum wells). For this reason, summing Eq. (45) over the final states, we obtain the transition rate W_i out of the state $|i\rangle$. This rate can be expressed in terms of the angular distribution $G(\theta)$:

$$W_i = \int_0^{2\pi} G(\theta) d\theta,$$

where

$$G(\theta) = \frac{k_f^-}{\epsilon_f'(k_f^-)} \int_{-\infty}^{\infty} N_{\mathbf{q}} R |\langle \psi_f(k_f^-) | e^{-i\mathbf{q}\mathbf{z}} | \psi_i(k_i) \rangle|^2 dq_z + \frac{k_f^+}{\epsilon_f'(k_f^+)} \int_{-\infty}^{\infty} (N_{\mathbf{q}} + 1) R |\langle \psi_f(k_f^+) | e^{i\mathbf{q}\mathbf{z}} | \psi_i(k_i) \rangle|^2 dq_z. \quad (46)$$

Here $q^2 = q_z^2 + q_{\parallel}^2$, $(\mathbf{k}_f - \mathbf{k}_i)^2 = q_{\parallel}^2 = k_f^2 + k_i^2 - 2k_f k_i \cos \theta$, the functions ψ_f and ψ_i do not depend on x and y and are solutions of the equation $H_0 \psi_n = \epsilon_n \psi_n$. The integrand $R(q) = e^2 \omega_0 / 2\pi \bar{\epsilon} q^2$ and $\epsilon_f'(k) = d\epsilon_f / dk$ (the index f indicates the number of the subband of the final state). For fixed k_i the wave vector k_f of the final state can be determined from the equation $\epsilon_i(k_i) - \epsilon_f(k_f^{\pm}) = \pm \hbar\omega_0$. A typical function $W_i(k_i)$, calculated on the basis of Eq. (46), is displayed in Fig. 4. The heterostructure parameters employed for these calculations are: $b_1 = 5.09$ nm, $b_2 = 12.44$ nm, $b_3 = 5.65$ nm; the aluminum concentrations in layers 1, 2, and 3 are 0, 0.0897, and 0.3, respectively; the temperature of the crystal $T = 77$ K. Each curve corresponds to transitions (marked by arrows) between subbands. At $k > k_1 = 25 \cdot 10^6$ cm⁻¹, the electron scattering rate increases abruptly, since above this value of the wave vector the energy conservation law allows the emission of a polar optical phonon. For $k < k_1$, the scattering is determined solely by the absorption of phonons, and it therefore approaches zero as $T \rightarrow 0$. The resonance tunneling point for this heterostructure lies at $k_* = 2 \cdot 10^6$ cm⁻¹. This was manifested as an intersection of all plots in the vicinity of k_* . It is evident from Fig. 4 that at $k \approx 0$, the intrasubband

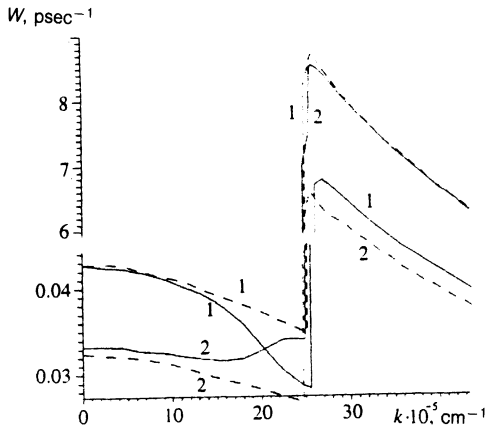


FIG. 5. Comparison of electron scattering rates by polar optical phonons for double-well (solid lines) and single-well (dashed lines) heterostructures.

transition rate is significantly lower than the intersubband-transition rate. This is directly related to the localization of electrons (belonging to a single energy subband in the initial and final states) in different quantum wells.

The rates of electron scattering by polar optical phonons in double-well (solid lines) and two single-well heterostructures (dashed lines) are compared in Fig. 5. The subbands for the double-well potential are denoted by 1 and 2, and on the dashed lines they correspond to the narrow and wide potential wells. Since the first quantum well is narrower, the corresponding transitions have a higher probability. Here the rate of scattering of 2D electrons by 3D phonons tends to increase as the well width decreases. This property results from the increase in the width of the domain of convergence of the integrals (46), since the matrix element appearing in the integrand is the Fourier transform of the probability density of an electron state localized in z . The rate of electron scattering by polar optical phonons has a finite upper limit at zero well width, while for acoustic phonons it approaches infinity. This difference is associated with the fact that $R(q)$ approaches zero for optical phonons and infinity for acoustic phonons in the limit $q \rightarrow \infty$. Far to the left and right of the synchronization point k_* the scattering rates for two wells and one well are close to one another, and upon traversal of a neighborhood of this point they change places. The normalized angular distribution $G(\theta)$ of polar optical phonons is shown in Fig. 6. It corresponds to radiative transitions within the first subband. Since $k_f^z = 0$ at $k_i = k_1$, this distribution is isotropic near k_1 . For larger values of k the probability of forward scattering increases.

We now study electron scattering by acoustic phonons. We employ the deformation-potential theory¹⁵ to determine the interaction Hamiltonian:

$$\hat{H}_{e-ac} = -i\Xi \sqrt{\frac{\hbar}{2Mc_a}} \sum_{\mathbf{q}} \sqrt{q} e^{i\mathbf{q}\cdot\mathbf{r}} (\hat{b}_{\mathbf{q}} - \hat{b}_{-\mathbf{q}}^+),$$

where Ξ is the deformation potential, M is the mass of the entire crystal, and c_a is the sound speed. Next, proceeding as in the case of polar optical phonons, we derive the ex-

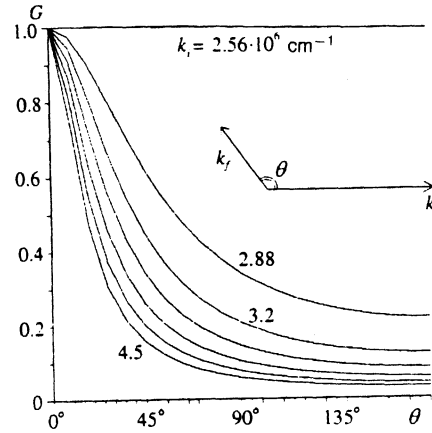


FIG. 6. Angular distribution of electrons with emission of polar optical phonons for a double-well potential.

pression (46) in which $R(q) = \Xi^2 q / 8\pi^2 \rho c_a$, where ρ is the density of the crystal. In contrast to the preceding case, the occupation number N_q of the phonon states cannot be removed from the integrand, since the phonon energy depends on the wave number $\hbar\omega_q = \hbar qc_a$. This is especially important for narrow potential wells, in which the domain of convergence of the integrals (46) as a function of q_z is wide. The rates of electron scattering by acoustic phonons in double- and single-well potentials at crystal temperatures of 4 and 77 K are compared in Fig. 7. The curves are numbered in the same manner as in Fig. 5. These figures are distinguished by the weak dependence of W_i for a single-well potential on the electron velocity at high crystal temperatures. Since all wave vectors lie near the center of the Brillouin zone, the energies of the acoustic phonons are significantly lower than the energies of the optical phonons and the average electron kinetic energy. Therefore $k_i \approx k_f$ and $\psi_i \approx \psi_f$. At high temperatures $N_q \approx k_B T / \hbar qc_a \gg 1$, and the integrals in Eq. (46) are identical. Since for a single-well potential ψ is virtually independent of k and q drops out of the integrand, $W_i \approx \text{const}$. The dip near $k=0$ is associated with the suppression of the emission of acoustic phonons for low electron kinetic energies. As is evident from Fig. 7, this dip increases with decreasing well width, since for scattering in a narrow well, the average phonon energy is higher because the q_z component is larger. The behavior of the double-well dependence, just as in Fig. 5, is determined by the abrupt change in the eigenfunctions (20) and (31) near the synchronization point. The rate of interband electron scattering by acoustic phonons is shown in Fig. 8. The solid line represents a transition from the first to the second subband, and the dashed line represents the reverse transition. Here, the crystal temperature is 77 K. The maximum of this distribution near the resonance tunneling point arises because the overlap of the wave functions is greatest at this point, and the discontinuity at $k \approx 6 \cdot 10^5 \text{ cm}^{-1}$ depends on the width of the energy gap between the subbands. The normalized angular distribution for the emission of an acoustic phonon by an electron

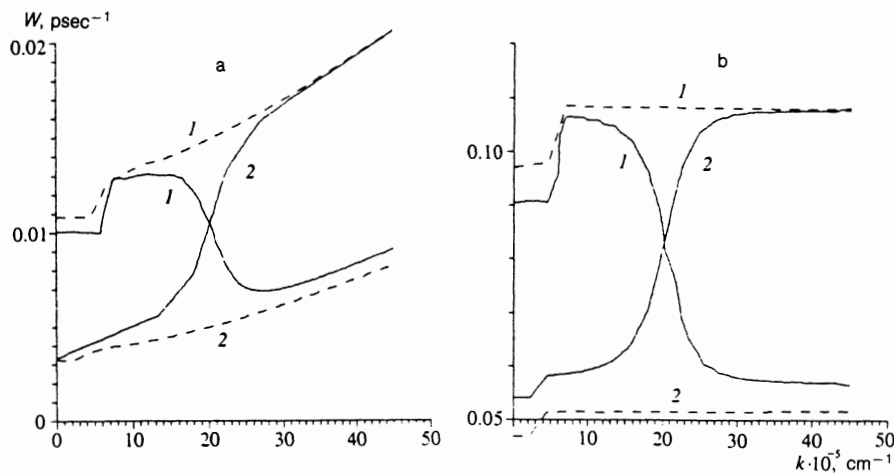


FIG. 7. Comparison of electron scattering rates by acoustic phonons for double-well (solid lines) and single-well (dashed lines) heterostructures. The crystal temperatures are 4 K (a) and 77 K (b).

at $T = 4 \text{ K}$ is displayed in Fig. 9. Scattering occurs within the first size-quantization subband. This distribution has a scattering maximum at 180° .

We use the model Hamiltonian

$$H_{e-\text{imp}} = \sum_i \delta(\mathbf{r} - \mathbf{r}_i)$$

to describe scattering by a neutral impurity. This Hamiltonian corresponds to a collection of delta-function-like force centers located at the points \mathbf{r}_i . Let the impurity be distributed randomly in some plane $z_{\text{imp}} = \text{const}$. Then the scattering is isotropic as a function of direction, and the electron transition rate from state $|i\rangle$ to state $|f\rangle$ is determined by the expression

$$W_{\text{imp}} = \frac{2\pi}{\hbar} |\langle \Psi_f(z_{\text{imp}}, k_f) | \Psi_i(z_{\text{imp}}, k_i) \rangle|^2 n_{\text{imp}} \delta(\epsilon_f - \epsilon_i), \quad (47)$$

where n_{imp} is the impurity concentration. In order that an electron be able to traverse the neighborhood of the synchronization point in the ballistic mode, we assume that $W_{\text{imp}}(k_i) = 0$ for $k_i \geq k_{\text{imp}} = 15 \cdot 10^6 \text{ cm}^{-1}$. Thus we employ

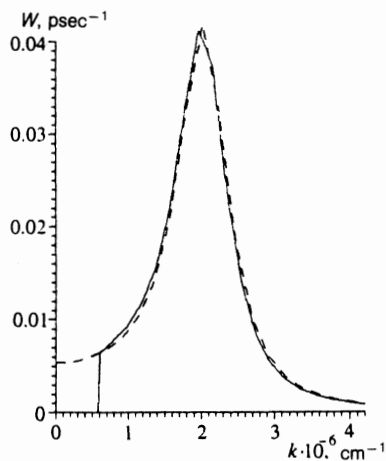


FIG. 8. Rate of interband electron scattering by acoustic phonons.

here the model of a resonance impurity that scatters electrons at low kinetic energy, far from the resonance tunneling energy.

5. CALCULATION OF THE CONDUCTIVITY OF A HETEROSTRUCTURE

In this paper, in order to neglect the electron-electron interaction, we assume that the electron distribution is uniform in the (xy) plane and the electron surface density is low. Landau-Zener tunneling gives rise to nonstationary states, and electron scattering by phonons and impurities transfers electrons into stationary states. The usual definition of the distribution function $f_s(k_x, k_y)$ and the kinetic equation are not suitable here, since they neglect stationary states. Let $f_s(k_{x0}, k_y, t)$ be the distribution of stationary states in the s th subband. Then the distribution function $\tilde{f}_s(k_{x0}, k_y, t)$ of the nonstationary electronic states in \mathbf{k} space is determined by the transport equation (9) and electron losses due to scattering:

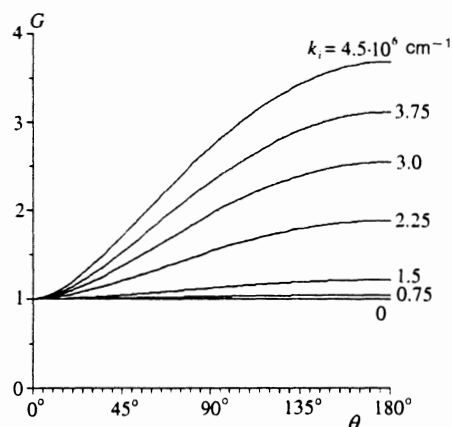


FIG. 9. Angular distribution for the emission of an acoustic phonon by an electron.

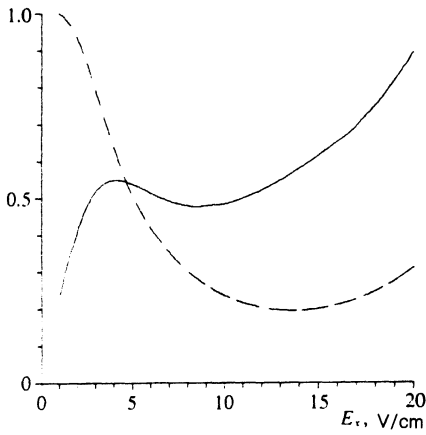


FIG. 10. Average electron velocity $v \times 10^{-7}$ cm/s (solid line) and probability P_1 of finding an electron in the first subband (dashed curve) as a function of longitudinal electric field strength.

$$\begin{aligned} \tilde{f}_s(k_x, k_y, t) = & \int_{-\infty}^{\infty} dk_{x0} \sum_i f_i \left(k_{x0}, k_y, t - \frac{\hbar(k_x - k_{x0})}{eE_x} \right) \\ & \times \exp \left(-\frac{\hbar}{eE_x} \int_{k_{x0}}^{k_x} \sum_j |c_{ij}(k_{x0}, k'_x, k_y)|^2 \right. \\ & \left. \times W_j(k_y, k'_x) dk'_x \right) |c_{is}(k_{x0}, k_x, k_y)|^2, \end{aligned} \quad (48)$$

where W_j is the transition rate from the j th subband, c_{ij} is the solution of Eq. (9) where the time t is replaced by k_x according to Eq. (7), and $c_{ij}(k_{x0}, k_{x0}, k_y) = \delta_{ij}$. The solutions satisfying these initial conditions can be easily expressed in terms of a system of fundamental solutions of Eq. (9), $Q_i(k_x, k_y)$, $i = 1, 2$, which satisfy the initial condition

$$Q_1(0, k_y) = 1, \quad Q_2(0, k_y) = 0$$

for all k_y . Following the derivation of Eq. (40) we obtain

$$\begin{aligned} c_{ij}(k_{x0}, k_x, k_y) = & Q_i^*(k_{x0}, k_y) Q_j(k_x, k_y) \\ & + (-1)^{i+j} Q_i(k_{x0}, k_y) Q_j^*(k_x, k_y), \end{aligned} \quad (49)$$

where $i, j = 1, 2$ and the overbar on a subscript denotes its complement, i.e., $\bar{i} = 3 - i$. Writing out the electron transition rate out of and into stationary states, we obtain the equation of balance of the states. This is the kinetic equation for the function f_s :

$$\begin{aligned} \frac{eE_x}{\hbar} f_s(k_{x0}, k_y, t) = & \sum_i \int_{-\infty}^{\infty} dk'_{x0} \int_{k_{x0}}^{\infty} dk'_x \int_{-\infty}^{\infty} dk'_y f_i \\ & \times \left(k'_{x0}, k'_y, t - \frac{\hbar(k'_x - k'_{x0})}{eE_x} \right) \exp \left(-\frac{\hbar}{eE_x} \right. \end{aligned}$$

$$\begin{aligned} & \left. \times \int_{k_{x0}}^{k'_x} \sum_j |c_{ij}(k'_{x0}, k''_x, k'_y)|^2 W_j(k''_x, k'_y) dk''_x \right. \\ & \left. \times \sum_j |c_{ij}(k'_{x0}, k'_x, k'_y)|^2 W_j^{j \rightarrow s}{}_{k'_x k'_y \rightarrow k_{x0} k_y} \right). \end{aligned} \quad (50)$$

The total transition rate $W_j(k_x, k_y)$ out of the unmixed state j is obtained from the partial scattering rates $W_{k_x k_y \rightarrow k'_{x0} k'_y}^{j \rightarrow s}$ by summing over s and integrating over all k'_{x0} and k'_y . The kinetic equation (50) is a linear integral system with delay. The delay arises due to the finite transition time from a stationary state into a nonstationary state. This problem was solved numerically by a variant of the Monte Carlo method. The $I(V)$ characteristic and the probability P_1 of finding an electron in the first subband as a function of E_x are displayed in Fig. 10. The plot contains a section where the average electron velocity decreases with increasing strength of the longitudinal electric field applied to the heterostructure. Negative differential conductance should be observed on this section. This behavior is due to Landau-Zener tunneling from a narrow potential well to a wide quantum well containing an impurity, resulting in a decrease in average electron velocity.

We now give the basic physical parameters for this calculation. The temperature of the crystal is 4 K; the thicknesses of the layers of the GaAs/Al_{0.3}Ga_{0.7}As/Al_{0.1}Ga_{0.9}As heterostructure are 4.9, 7.2, and 13.84 nm, respectively; the wave vector of the synchronization point $k_* = 20 \cdot 10^6$ cm⁻¹, and the energy gap at this point $\delta\varepsilon_* = 0.23$ meV. Table I gives the number of electron scattering events occurring for different scattering mechanisms within $4 \cdot 10^{-6}$ sec in an electric field $E_x = 11.5$ V/cm. The number of transitions out of nonstationary states was determined according to Eq. (14) and is given in Table I. It is evident from these results that the dominant mechanism is impurity scattering within the second subband. Since this occurs for $k < 1.5 \cdot 10^6$ cm⁻¹, an electron with relatively low average velocity spends most of its time in this region. Emission of acoustic phonons in the first subband is a secondary process. The probability of emission of an acoustic phonon in a narrow layer of width b is proportional to $1/b^2$. This imposes a lower limit on the width of the GaAs layer, since this mechanism prevents ballistic transport in the vicinity of the resonance tunneling point.

Transitions due to electron scattering by polar optical phonons within the second subband (2→2) are absent because there is enough time for an electron to complete a transition in the first three scattering channels (see Fig. 4). In stronger electric fields this channel comes into play. The channel 1→2 transfers electrons undergoing Landau-Zener tunneling into the second subband near $k \approx 0$. This transition is therefore responsible for the section with negative differential conductance. This section vanishes when the channel is artificially closed.

6. CONCLUSIONS

In this work the parameters of the quantum wells in the heterostructure were specially selected so as to guaran-

TABLE I. Number of electron scattering events in a double-well heterostructure during the acquisition time of a statistical sample.

Transitions	Emission of polar optical phonons	Emission of acoustic phonons	Absorption of acoustic phonons	Impurity
1 → 1	574	13141	529	5
1 → 2	1294	464	9	354
2 → 1	1235	240	20	1721
2 → 2	0	11371	2368	501354

tee the existence of a section with negative differential conductance in a longitudinal electric field. The following conditions had to be taken into account:

- the existence of two weakly coupled energy subbands $\varepsilon_{1,2}(k)$ with a synchronization point k_* , and $\varepsilon_{1,2}(k_*) - \varepsilon_1(0) < \hbar\omega_0$, where $\hbar\omega_0$ is the energy of the polar optical phonons;
- the existence of an impurity in the higher quantum well;
- weak overlap of the wave functions in regions far from the synchronization point; and,
- the rates of electron scattering by phonons and impurities must be low enough that transport through the synchronization point is ballistic.

These conditions are mutually inconsistent, so a compromise must be sought. For example, the third condition might be satisfied by prescribing a sufficiently high barrier between the wells. In this case, however, the tunneling time increases, and this will cause the fourth condition to be violated. Appropriate heterostructure parameters yielding the best result probably exist for each specific regime.

- ¹N. Vodjdani, B. Vinter, V. Berger *et al.*, Appl. Phys. Lett. **59**, 555 (1991).
- ²D. H. Levi, Phys. Rev. B **45**, 4274 (1992).
- ³D. Ahn, IEEE J. Quantum Electron. **25**, 2260 (1989).
- ⁴T. B. Norris, N. Vodjdani, B. Vinter *et al.*, Phys. Rev. B **40**, 1392 (1989).
- ⁵V. L. Borblik, Z. S. Gribnikov, and B. P. Markevich, Fiz. Tekh. Poluprovodn. **25**, 1302 (1991) [Sov. Phys. Semicond. **25**, 786 (1991)].
- ⁶V. J. Goldman, D. C. Tsui, and J. E. Cunningham, Phys. Rev. Lett. **58**, 1256 (1987).
- ⁷L. D. Landau and E. M. Lifshitz, *Quantum Mechanics*, Pergamon Press, New York (1977).
- ⁸C. Zener, Proc. Roy. Soc. Lond. Ser. A **137**, 696 (1932).
- ⁹R. I. Cukier, M. Morillo, and J. M. Casado, Phys. Rev. B **45**, 1213 (1992).
- ¹⁰V. R. Gushchin, Zh. Eksp. Teor. Fiz. **100**, 924 (1991) [Sov. Phys. JETP **73**, 510 (1991)].
- ¹¹J. A. Alamo and C. C. Eugster, Appl. Phys. Lett. **56**, 78 (1990).
- ¹²R. Q. Yang and J. M. Xu, Appl. Phys. Lett. **59**, 315 (1991).
- ¹³R. Ferreira and G. Bastard, Phys. Rev. B **40**, 1074 (1989).
- ¹⁴B. K. Ridley, *Quantum Processes in Semiconductors*, Oxford University Press, New York (1993).
- ¹⁵A. S. Davydov, *Theory of the Solid State* [in Russian], Nauka, Moscow, 1976.

Translated by M. E. Alferieff